Thomas Jefferson University
Jefferson Digital Commons

Wills Eye Hospital Papers | Wills Eye Hospital

4-3-2023

Identification of the Vibrational Optical Coherence Tomography Corneal Cellular Peak

Nathalie D. Daher
Thomas Jefferson University

Ahmed Saeed Saad
Thomas Jefferson University

Hiram J. Jimenez
Thomas Jefferson University

Tatyana Milman
Thomas Jefferson University

Orlando G. Gonzalez-Martinez

Follow this and additional works at: https://jdc.jefferson.edu/willsfp

Part of the Ophthalmology Commons

Let us know how access to this document benefits you

Recommended Citation

Daher, Nathalie D.; Saad, Ahmed Saeed; Jimenez, Hiram J.; Milman, Tatyana; Gonzalez-Martinez, Orlando G.; Deshmukh, Tanmay S.; Pulido, Jose S.; Silver, Frederick H.; Benedetto, Dominick A.; Rapuano, Christopher J.; and Syed, Zeba A., "Identification of the Vibrational Optical Coherence Tomography Corneal Cellular Peak" (2023). *Wills Eye Hospital Papers.* Paper 180.
https://jdc.jefferson.edu/willsfp/180

This Article is brought to you for free and open access by the Jefferson Digital Commons. The Jefferson Digital Commons is a service of Thomas Jefferson University's Center for Teaching and Learning (CTL). The Commons is a showcase for Jefferson books and journals, peer-reviewed scholarly publications, unique historical collections from the University archives, and teaching tools. The Jefferson Digital Commons allows researchers and interested readers anywhere in the world to learn about and keep up to date with Jefferson scholarship. This article has been accepted for inclusion in Wills Eye Hospital Papers by an authorized administrator of the Jefferson Digital Commons. For more information, please contact: JeffersonDigitalCommons@jefferson.edu.

Authors

Nathalie D. Daher, Ahmed Saeed Saad, Hiram J. Jimenez, Tatyana Milman, Orlando G. Gonzalez-Martinez, Tanmay S. Deshmukh, Jose S. Pulido, Frederick H. Silver, Dominick A. Benedetto, Christopher J. Rapuano, and Zeba A. Syed

This article is available at Jefferson Digital Commons: https://jdc.jefferson.edu/willsfp/180

tvst

Cornea & External Disease

Identification of the Vibrational Optical Coherence Tomography Corneal Cellular Peak

Nathalie D. Daher[1,*], Ahmed Saeed Saad[1,*], Hiram J. Jimenez[2,*], Tatyana Milman[3], Orlando G. Gonzalez-Martinez[3], Tanmay Deshmukh[4], Jose S. Pulido[2], Frederick H. Silver[4,5], Dominick A. Benedetto[6], Christopher J. Rapuano[1], and Zeba A. Syed[1]

[1] Cornea Service, Wills Eye Hospital, Sidney Kimmel Medical College at Thomas Jefferson University, Philadelphia, PA, USA
[2] Vickie and Jack Farber Vision Research Center, Wills Eye Hospital, Philadelphia, PA, USA
[3] Pathology Department, Wills Eye Hospital, Sidney Kimmel Medical College at Thomas Jefferson University, Philadelphia, PA, USA
[4] OptoVibronex, LLC., Bethlehem, PA, USA
[5] Department of Pathology and Laboratory Medicine, Robert Wood Johnson Medical School, Rutgers, the State University of New Jersey, Piscataway, NJ, USA
[6] Center for Advanced Eye Care, Vero Beach, FL, USA

Correspondence: Zeba A. Syed, Sidney Kimmel Medical College at Thomas Jefferson University, Cornea Service, Wills Eye Hospital, 840 Walnut Street, Suite 920, Philadelphia, PA 19107, USA.
e-mail: zsyed@willseye.org

Received: December 25, 2022
Accepted: February 26, 2023
Published: April 12, 2023

Keywords: cornea; biomechanics; vibrational OCT; mechanical properties

Citation: Daher ND, Saad AS, Jimenez HJ, Milman T, Gonzalez-Martinez OG, Deshmukh T, Pulido JS, Silver FH, Benedetto DA, Rapuano CJ, Syed ZA. Identification of the vibrational optical coherence tomography corneal cellular peak. Transl Vis Sci Technol. 2023;12(4):11, https://doi.org/10.1167/tvst.12.4.11

Purpose: Our team previously identified the presence of five corneal resonant frequency (RF) peaks in healthy volunteers using vibrational optical coherence tomography (VOCT). Prior studies have suggested that the $\leq$100 Hz RF peak represents the cellular element of tissue. The aim of this study was to confirm that this peak reflects the human corneal cellular component using VOCT and histological analysis.

Methods: Two human research globes were obtained from the same donor, and VOCT measurements were collected from the full-thickness corneas. A microkeratome was then used to create serial-free corneal caps from each cornea, with VOCT performed on the residual stromal bed after each excision. All lamellar sections from both globes were sent for histological analysis to determine cellularity. Cell counts on the specimens were performed by two independent observers.

Results: The average of the normalized $\leq$100 Hz peak values before lamellar sectioning was significantly higher than the average of this peak values after the first, second, and third cuts ($P = 0.023$), which was 33.9% less than before any cuts. The cell count values in the first slice were significantly higher than the average cell count values of the three deeper slices ($P < 0.001$), and the cell count dropped 84.4% after the first slice was removed.

Conclusions: The findings of this study suggest that the $\leq$100 Hz corneal peak identified by VOCT corresponds to the cellular component of the cornea.

Translational Relevance: This work furthers our understanding of the origin of the corneal $\leq$100 Hz peak identified using VOCT.

Introduction

Conditions associated with altered corneal biomechanics include keratoconus and other ectasias,[1,2] refractive surgery,[3] alkali burn,[4] and glaucoma.[5] Various diagnostic modalities are available to measure corneal biomechanics in vivo including Ocular Response Analyzer (Reichart Ophthalmic Instruments, Buffalo, NY, USA) and Corneal Visualization Scheimpflug Technology (Corvis ST; Oculus Optikgeräte GmbH, Wetzlar, Germany).[6] Although these two devices are currently widely marketed and used, their measurements vary according to characteristics of adjacent tissues such as anterior chamber volume, aqueous humor movement, iris and lens

Copyright 2023 The Authors

This work is licensed under a Creative Commons Attribution-NonCommercial-NoDerivatives 4.0 International License.

Downloaded from tvst.arvojournals.org on 05/05/2023

anatomy, and intraocular pressure fluctuation.[7–12] Additional technology that can measure corneal biomechanical properties include magnetic resonance elastography, optical coherence elastography, and Brillouin optical microscopy.[13–16] Among ex vivo methods, the most widely used to measure stress-strain behavior is corneal strip extensometry.[17–19]

Vibrational optical coherence tomography (VOCT) is a noninvasive and nondestructive device that measures resonant frequency (RF) and the elastic modulus of the components of tissue under examination. VOCT has been used to measure the biomechanical (including elastic and viscous) properties of different materials.[20–24] A spectrum of audible sound waves is used to vibrate tissue in conjunction with simultaneous imaging by optical coherence tomography (OCT).[20,25–29] Through the OCT, an infrared light detects the tissue displacement and measures the RF,[25–28] which is the frequency at which the maximum displacement is achieved.[20,23,24] Our team recently published findings from the in vivo use of VOCT to evaluate corneas of healthy human volunteers and 5 RF peaks were identified.[30] This pilot study demonstrated that the first peak noted in the lowest frequency range of $\leq$100 Hz had a mean RF of 73.5 $\pm$ 4.9 Hz in the central cornea and a mean RF of 72.1 $\pm$ 6.3 Hz in the inferior cornea.[30]

Previous studies have suggested that the RF of the cellular component of skin is similarly $\leq$100 Hz.[21,22,31–35] Based on prior literature, we hypothesize that the $\leq$100 Hz peak in human corneas corresponds to their cellular component. In this study, we confirm this speculation using VOCT and histology of lamellar sections and emphasize the utility of VOCT as a novel technology to characterize corneal biomechanics.

Methods

This prospective study was performed in compliance with the Health Insurance Portability and Accountability Act (HIPAA), adhered to the tenets of the Declaration of Helsinki, and was approved by the Wills Eye Hospital Institutional Review Board.

Acquisition and Preparation of Globes

Two human globes from the same donor were obtained for research purposes (Eversight, Ann Arbor, MI, USA). The globes were from a 70-year-old Caucasian female. The time from death to preservation was 18 hours, and the globes were received by our facility 45 hours after death. The patient had no history of ocular disease (including keratoconus and glaucoma) or any prior ocular surgeries.

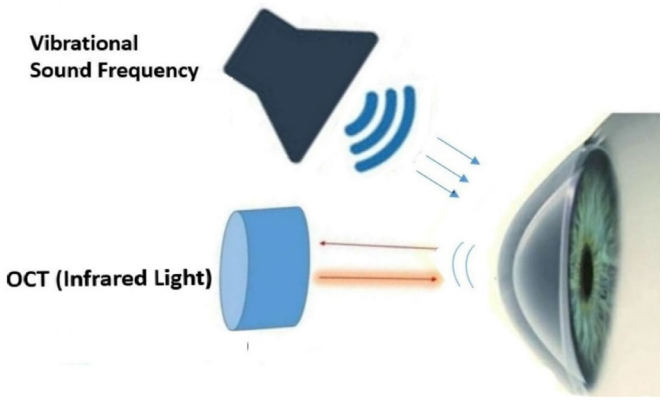

Figure 1. Schematic representation of the VOCT technique. Sound waves are produced by the speaker (approximately 1–2 inches away from the cornea for this experiment) and causes displacement of the corneal tissue, which is detected through OCT using infrared light. A photograph of the machine's setup has been previously published.[30]

Immediately on the arrival of the paired fresh globes, each was placed in the orbital cavity of a mannequin head according to its original anatomical orientation. The intraocular pressure was monitored with a Tonopen (Reichert Technologies, Buffalo, NY, USA) and maintained at 15 to 20 mm Hg through an intravitreal injection of balanced saline solution at the temporal pars plana with a 30-gauge needle.

VOCT Measurements

The VOCT measurements were collected from the full thickness corneas of each globe after fixating the globes in a mannequin head in front of the VOCT device such that the acoustic Bluetooth speaker (EWA A106 Pro; J.Y.M. Digital Technology Co., Ltd, Shenzhen, Guangdong, China) and OCT (Lumedica Inc., Durham, NC, USA) measured the central cornea of the globes without direct contact. We scanned each eye at the center of the cornea, because we recognize that corneal thickness and collagen density and distribution may differ between the central and peripheral cornea.

Figure 1 illustrates a simplified schematic representation of the VOCT device and procedure. The technique for VOCT measurements of the donor globes was similar to that previously described for human subjects,[30] which uses a Bluetooth speaker capable of producing audible driving frequencies between 30 and 250 Hz at an amplitude of 55 decibels that cause displacement of tissue components under examination. This displacement is then detected by a spectral-domain OCT system (operating in A-mode) using infrared light (840 nm). The RF is obtained by noting the frequency at which the maximum tissue displacement is achieved and is dependent on the material thickness.[20,23,24]

Downloaded from tvst.arvojournals.org on 05/05/2023

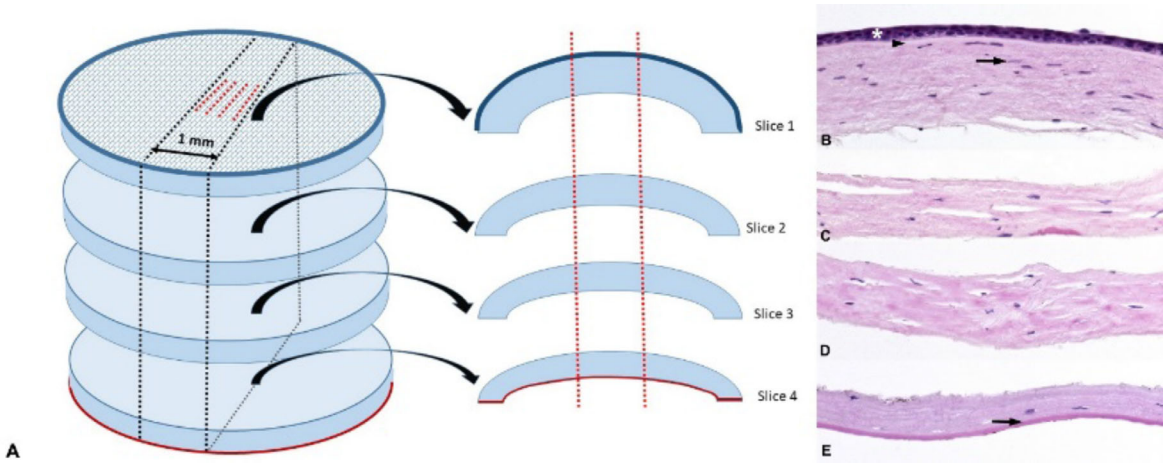

Figure 2. Schematic model of cell count analyses. (A) Each lamellar slice was sectioned to sample the central 1 mm of tissue (*black dotted lines*), and four levels within each 1 mm section (*red dotted lines*) were analyzed. Representative histological images from the first (B), second (C), third (D), and fourth (E) lamellar slices. *Asterisk* indicates the epithelium; *arrowhead* indicates the Bowman membrane; *arrow* indicates (B) the keratocyte; and *arrow* indicates (E) the Descemet membrane (hematoxylin-eosin stain; magnification × 100).

Lamellar Corneal Sectioning

A Moria Evolution 3 unit (Moria, Antony, France) with a Carriazo Barraquer (CB) single-use microkeratome 110 head, CBm turbine, and suction ring were used to create free corneal caps from each cornea of the paired globes. Each lamellar slice was approximately 110 µm in thickness. The CB microkeratome head was screwed into the turbine. The metallic suction ring was centered on the corneal-scleral junction, allowing the microkeratome blade to enter the cornea. The vacuum was initiated to stabilize the globe during the passage of the microkeratome blade through the cornea. The foot pedal was engaged while allowing the microkeratome head to move in a single consistent motion to complete the pass in approximately five seconds.

A central corneal 8 mm diameter free lamellar cap was created and submitted for histological study. After removing the suction ring, the intraocular pressure was adjusted as described previously. After removal of the first lamellar cap, VOCT measurements were performed on the remaining corneal stromal bed. This process was repeated to create the second and third lamellar caps. The fourth corneal cap was the last created for both globes as the anterior chamber was entered during passage of the blade.

Cellular Count Measurements

After lamellar corneal sectioning, each slice was fixed in 10% buffered formaldehyde. Sections of 5 µm thickness were prepared from the routinely processed paraffin-embedded tissues. Figure 2 presents a schematic model of histological analyses. Each cornea was submitted as four distinct lamellae as described above. All slices were sectioned sequentially from their nasal to temporal margins, sampling the central 1 mm of corneal tissue at step levels (Fig. 2A). One hundred eighty sections were stained with hematoxylin-eosin and examined. Corneal epithelium, Bowman layer, stroma, and Descemet membrane were morphologically unremarkable. Corneal endothelium was artifactitiously denuded, which was likely secondary to manipulation during lamellar segmentation and during orientation and sectioning for pathology. Less likely, but it is also possible that some endothelial cell loss occurred during the interval between time of death to fixation. Representative stained sections sampling four 200 to 250 µm levels in the central 1 mm of each slice were scanned with MoticEasyScan virtual slide scanner (Motic Digital Pathology, Vancouver, Canada) and displayed via Aperio ImageScope viewer (Leica Biosystems, Nussloch, Germany).

Corneal epithelial and stromal keratocyte cell counts were performed by two independent observers (T.M., O.G.G.) on four representative levels from the 1 mm central cross-section of each slice (Figs. 2B–E), and counts were averaged for each slice.

Statistical Analysis

Descriptive statistics were used for VOCT and histological results, and Student's *t*-tests were used to identify significant differences between the samples. P values < 0.05 were considered to be statistically

Downloaded from tvst.arvojournals.org on 05/05/2023

significant. Data were analyzed using Microsoft Excel (Microsoft Inc., Redmond, WA, USA).

Results

Analysis of VOCT Measurements in Lamellar Slices

When the donor corneas were evaluated using VOCT prior to lamellar sectioning, the 5 previously-published peaks were observed (Figs. 3, 4).[30] We focused on the peak with a RF of ≤100 Hz and normalized the VOCT data in each examination by dividing the height of each peak value by the peak with the highest weighted displacement. Weighted displacement accounts for corrections to the peaks after speaker vibrations without a sample present are removed from the raw data. The peak heights will vary depending on the speaker distance from the cornea and exact angle of the speaker, and these differences are corrected by normalization.

As presented in Table 1, after data normalization the value of the ≤100 Hz peak was 1.0 in both globes before lamellar sectioning. The peak dropped to 0.552 and 0.764 after cutting the first lamellar slice, 0.538 and 0.500 after cutting the second lamellar slice, and 0.636 to 0.975 after cutting the third lamellar slice.

The average normalized ≤100 Hz peak value before lamellar sectioning was significantly higher than the average of this peak's values after the first, second, and third cuts (1.0 vs. 0.661, $P = 0.023$), and the ≤100 Hz peak decreased 33.9% after the first lamellar cut. None of the other four preidentified corneal peaks[30] showed a statistically significant decrease after the first lamellar cut ($P > 0.05$ for all). The diminution of the ≤100 Hz peak after removal of the most superficial layer is demonstrated in the right globe in Figure 3 and left globe in Figure 4.

Cellular Counts in Individual Corneal Layers

Averaging the measurements obtained by two observers using four levels of each tissue specimen from two globes, the average cell count measured for the first lamellar section was 276.5 ± 10.3, which consisted of an average of 203.6 epithelial cells and 72.9 keratocytes. The second, third, and fourth slices had average cell counts of 49.5 ± 1.5, 48.3 ± 7.4, and 31.5 ± 5.6, respectively. As described above, endothelial cells were artifactitiously denuded and thus not included in the count. Table 2 details the cell count values from each slice for the two globes.

The mean epithelial cell and keratocyte cell counts obtained by the two observers in the most superficial slice were compared with the mean keratocyte cell count values of the other three slices. The average cell count values in the first slice were significantly higher than the average cell count values of the three deeper slices (276.5 vs. 43.1, $P < 0.001$), and the cell count dropped 84.4% after the first cut. Given that the reduction in the ≤100 Hz peak corresponded to the

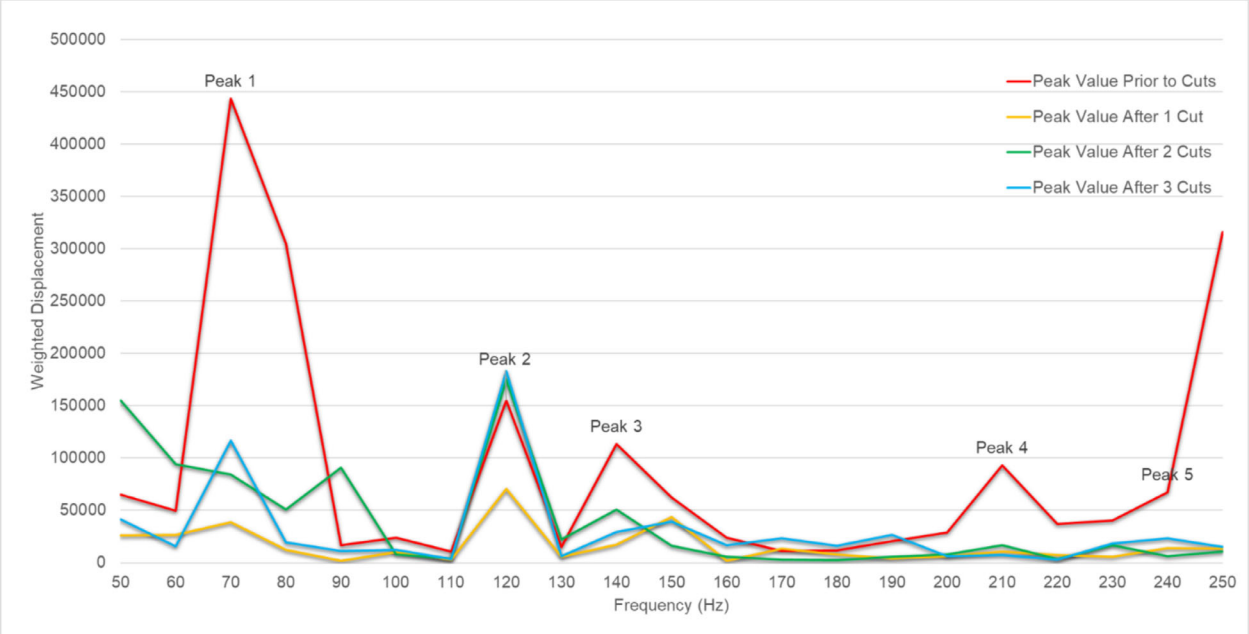

Figure 3. Frequency versus weight displacement for the right donor globe before and after each lamellar section.

translational vision science & technology

Downloaded from tvst.arvojournals.org on 05/05/2023

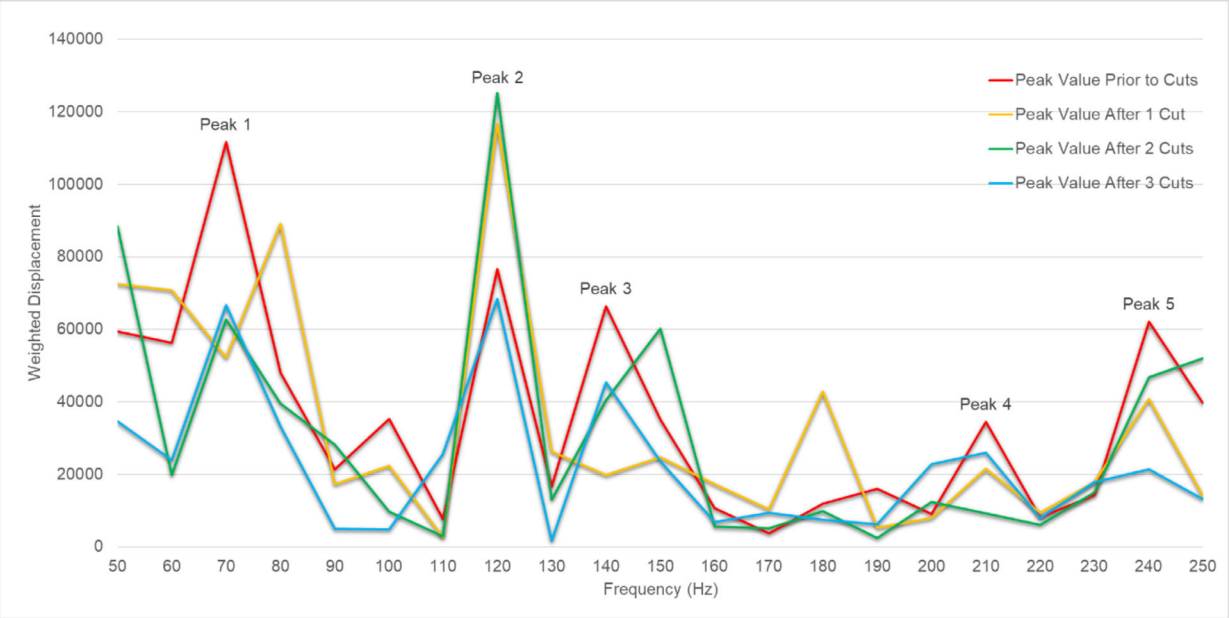

Figure 4. Frequency versus weight displacement for the left donor globe before and after each lamellar section.

Table 1. Normalized Values for the ≤100 Hz Peak Before and After Lamellar Sectioning

Peak 1	Resonant Frequency (Hz)	Normalized Peak 1 Value Right Globe	Normalized Peak 1 Value Left Globe	Average ($P = 0.023$)
Before cuts	≤100	1.0	1.0	1.0
After Cut 1	≤100	0.552	0.764	0.661
After Cut 2	≤100	0.538	0.500	
After Cut 3	≤100	0.636	0.975	

Table 2. Cell Count for Each Human Donor Cornea Tissue From Two Observers

	Cell Count (Mean ± SD)				
Cornea Tissue	Observer 1 Right Globe	Observer 1 Left Globe	Observer 2 Right Globe	Observer 2 Left Globe	Average ($P < 0.001$)
Slice 1	287.3 ± 37.5	269.0 ± 16.4	286.0 ± 49.5	263.8 ± 26.2	276.5
Slice 2	51.0 ± 4.7	48.0 ± 11.2	50.5 ± 5.4	48.5 ± 12.1	43.1
Slice 3	55.0 ± 9.6	41.0 ± 3.3	54.3 ± 12.3	42.8 ± 4.6	
Slice 4	27.0 ± 6.3	37.0 ± 6.5	26.3 ± 8.7	35.5 ± 5.2	

removal of the most anterior section of the cornea, which includes the epithelium and superficial stroma, we conclude that this peak reflects the human corneal cellular component.

Discussion

Previous VOCT studies have demonstrated that the cellular contributions of skin have a RF ≤100 Hz,[21,22,31–35] which would correspond to the lowest RF peak previously obtained from in vivo human corneas.[30] Higher RF values were attributed to collagen fibers of normal dermis.[21,22,31–35] Silver et al.[31] analyzed different tissues in vivo using VOCT and showed that normal skin has resonant frequency peaks at 50 to 70 Hz, 100 to 120 Hz, and 150 Hz corresponding to the cellular epidermal component (50–70 Hz), collagenous dermal components (100–120 Hz), and extracellular matrix in the arterial wall (150 Hz). Additional evidence that the ≤100 Hz RF peak represents the cellular component of tissue was published in a study highlighting VOCT's potential to perform "virtual biopsies" of skin after thermal and chemical burns.[32] A study analyzing skin lesions with VOCT found a value of 50 Hz as the RF for the cellular components.[34]

Our study supports the hypothesis that the cellular component of the human cornea corresponds to the ≤100 Hz peak, one of the five peaks identified using VOCT in normal human corneas.[30] Although the relative heights of these five peaks differed in the current study compared to our pilot study,[30] the peaks with higher RF values may represent extracellular tissue components that may be affected by periocular tissue present in the human volunteers included in the pilot study. With our histological analyses, we demonstrated that the number of cells is higher in the anterior layers of the cornea, because average cell count measurements dropped 84.4% after removal of the most superficial slice of the cornea. It is known that the epithelial cell layer and anterior stroma contain the vast majority of cells within the cornea.[36] Removal of

Downloaded from tvst.arvojournals.org on 05/05/2023

this anterior layer corresponded to a 33.9% reduction in the ≤100 Hz peak height, suggesting that cells are the most important contributor to the first weighted displacement in this layer. Of note, the ≤100 Hz peak identified with VOCT included endothelial cells, which were absent from histological analysis, likely because of loss during experimentation or processing. This phenomenon may partly explain why the percent reduction in cell count measurement was higher than the drop in the corresponding peak height.

The clinical implications of this study involve the potential utility of VOCT to measure epithelial changes as a marker of keratoconus severity. Previous studies have demonstrated that alternations in the epithelial layer occur early in this disease.[37] Basal epithelial cells in patients with keratoconus may undergo enlargement, irregular arrangement, and a decrease in cell density.[38–40] Interestingly, the epithelial remodeling that occurs in keratoconus is so striking that it may independently differentiate normal from diseased eyes.[41] Further research is needed to validate our findings and to determine the role of VOCT in grading keratoconus severity based on epithelial features. Studies are also needed to understand VOCT changes in conditions involving corneal edema. In the field of dermatology, this technology has been used to analyze biomechanical features of human skin,[25–27,34] to characterize malignant and premalignant skin lesions,[21] chemical and burn wounds,[32] and for performing a "virtual biopsy" of skin lesions.[32,33]

The current study has several limitations. Our sample size was small with only two globes analyzed. However, our results are consistent with other studies discussed above,[21,22,31–35] and we have previously demonstrated the repeatability of VOCT findings.[30] Our examination of the material prepared for histology in the study could be affected by changes that occur during formalin fixation, processing, and preparation of the sample, as was the case with endothelial cells. We noticed that in the left globe, the height of the ≤100 Hz VOCT peak increased after the third cut (Table 1). The height of this peak includes the corneal endothelium that is concentrated in this section after the rest of the cornea is removed. The original content and retention of the intact endothelium during processing will affect this peak after the third cut. As a result, we anticipate there to be variation between eyes, because both eyes are not identical. Furthermore, there may be "noise" in each individual eye's normalized VOCT data, because each peak is divided by the highest peak from that particular study. In the case of the left globe after the third cut, there may have been variable heights for the remaining four peaks, resulting in a higher normalized first peak. This "noise" was the primary reason we took the average of both eyes in our analysis. Finally, RF values obtained with VOCT have a margin of error of ± 10 Hz, limiting the accuracy of identified peaks.[21]

In this study, we demonstrate that VOCT can effectively isolate the cellular component of corneal tissue. Further studies are needed to understand whether alterations occur in the ≤100 Hz VOCT peak in corneal pathology, such as keratoconus, and whether VOCT can assist in clinical management as has been the case in dermatology.[21,31–34] Future experimental studies with VOCT are planned to identify the origin of other RF peaks identified in the cornea with the goal of studying early biophysical markers of corneal disease.

Acknowledgments

Supported by BNY Mellon and the Elizabeth C. King Trust.

Disclosure: **N.D. Daher**, None; **A.S. Saad**, None; **H.J. Jimenez**, None; **T. Milman**, None; **O.G. Gonzalez-Martinez**, None; **T. Deshmukh**, OptoVibronex, LLC (E); **J.S. Pulido**, None; **F.H. Silver**, OptoVibronex, LLC (P); **D.A. Benedetto**, OptoVibronex, LLC (C); **C.J. Rapuano**, None; **Z.A. Syed**, None

* ND, AS, and HJ are co-first authors who contributed equally to the preparation of this work.

References

1. Ortiz D, Piñero D, Shabayek MH, Arnalich-Montiel F, Alió JL. Corneal biomechanical properties in normal, post-laser in situ keratomileusis, and keratoconic eyes. *J Cataract Refract Surg.* 2007;33:1371–1375.
2. Sinha Roy A, Shetty R, Kummelil MK. Keratoconus: A biomechanical perspective on loss of corneal stiffness. *Indian J Ophthalmol.* 2013;61:392–393.
3. González-Méijome JM, Villa-Collar C, Queirós A, Jorge J, Parafita MA. Pilot study on the influence of corneal biomechanical properties over the short term in response to corneal refractive therapy for myopia. *Cornea.* 2008;27:421–426.
4. Mekonnen T, Lin X, Zevallos-Delgado C, et al. Longitudinal assessment of the effect of alkali burns on corneal biomechanical properties using optical coherence elastography. *J Biophotonics.* 2022;15(8):e202200022.
5. Grise-Dulac A, Saad A, Abitbol O, et al. Assessment of corneal biomechanical properties in normal tension glaucoma and comparison with

translational vision science & technology

Downloaded from tvst.arvojournals.org on 05/05/2023

open-angle glaucoma, ocular hypertension, and normal eyes. *J Glaucoma*. 2012;21:486–489.
6. Garcia-Porta N, Fernandes P, Queiros A, Salgado-Borges J, Parafita-Mato M, González-Méijome JM. Corneal biomechanical properties in different ocular conditions and new measurement techniques. *ISRN Ophthalmol.* 2014;2014:724546.
7. Luce DA. Determining in vivo biomechanical properties of the cornea with an ocular response analyzer. *J Cataract Refract Surg*. 2005;31:156–162.
8. Kling S, Marcos S. Contributing factors to corneal deformation in air puff measurements. *Invest Ophthalmol Vis Sci*. 2013;54:5078–5085.
9. Alonso-Caneiro D, Karnowski K, Kaluzny BJ, Kowalczyk A, Wojtkowski M. Assessment of corneal dynamics with high-speed swept source optical coherence tomography combined with an air puff system. *Opt Express.* 2011;19:14188–14199.
10. Dorronsoro C, Pascual D, Pérez-Merino P, Kling S, Marcos S. Dynamic OCT measurement of corneal deformation by an air puff in normal and cross-linked corneas. *Biomed Opt Express.* 2012;3:473–487.
11. Piñero DP, Alcón N. Corneal biomechanics: A review. *Clin Exp Optom.* 2015;98:107–116.
12. Lopes BT, Bao F, Wang J, et al. Review of in-vivo characterisation of corneal biomechanics. *Med Nov Technol Devices*. 2021;11:100073.
13. Manduca A, Oliphant TE, Dresner MA, et al. Magnetic resonance elastography: Non-invasive mapping of tissue elasticity. *Med Image Anal.* 2001;5:237–254.
14. Litwiller DV, Lee SJ, Kolipaka A, et al. MR elastography of the ex vivo bovine globe. *J Magn Reson Imaging.* 2010;32:44–51.
15. Ramier A, Eltony AM, Chen Y, et al. In vivo measurement of shear modulus of the human cornea using optical coherence elastography. *Sci Rep*. 2020;10(1):17366.
16. Scarcelli G, Pineda R, Yun SH. Brillouin optical microscopy for corneal biomechanics. *Invest Ophthalmol Vis Sci.* 2012;53:185–190.
17. Richoz O, Kling S, Zandi S, Hammer A, Spoerl E, Hafezi F. A constant-force technique to measure corneal biomechanical changes after collagen cross-linking. *PLoS One.* 2014;9(8):e105095.
18. Ruberti JW, Sinha Roy A, Roberts CJ. Corneal biomechanics and biomaterials. *Annu Rev Biomed Eng.* 2011;13:269–295.
19. Chang SH, Mohammadvali A, Chen KJ, et al. The relationship between mechanical properties, ultrastructural changes, and intrafibrillar bond formation in corneal UVA/riboflavin cross-linking treatment for keratoconus. *J Refract Surg.* 2018;34:264–272.
20. Silver F, Horvath I, Kelkar N, Deshmukh T, Shah R. In vivo biomechanical analysis of human tendon using vibrational optical coherence tomography: Preliminary results. *J Clin Cases Rep.* 2020;4:12–19.
21. Silver FH, Deshmukh T, Ryan N, Romm A, Nadiminti H. "Fingerprinting" benign and cancerous skin lesions using vibrational optical coherence tomography: Differentiation among cancerous lesion types based on the presence of new cells, blood vessels, and fibrosis. *Biomolecules*. 2022;12:1332.
22. Silver FH, Shah RG, Richard M, Benedetto D. Comparison of the virtual biopsies of a nodular basal cell carcinoma and an actinic keratosis: Morphological, cellular and collagen analyses. *Adv Tissue Eng Regen Med*. 2019;5(2):61–66.
23. Silver FH, Shah RG, Silver LL. The use of vibrational optical coherence tomography in matching host tissue and implant mechanical properties. *Biomater Med Appl.* 2018;2(2).
24. Silver FH, Shah RG. Analysis of the mechanical behavior of composite tissues using vibrational optical coherence tomography. *World J Mech.* 2017;7:271–282.
25. Shah RG, Pierce MC, Silver FH. Morphomechanics of dermis-A method for non-destructive testing of collagenous tissues. *Skin Res Technol.* 2017;23:399–406.
26. Silver FH, Silver LL. Non-invasive viscoelastic behavior of human skin and decellularized dermis using vibrational OCT. *Dermatology Clin Res*. 2017;3:174–179.
27. Shah RG, DeVore D, Silver FH. Biomechanical analysis of decellularized dermis and skin: Initial in vivo observations using optical cohesion tomography and vibrational analysis. *J Biomed Mater Res A*. 2018;106:1421–1427.
28. Silver FH, Silver LL. Use of vibrational optical coherence tomography in dermatology. *Arch Dermatol Skin Care.* 2018;1(2):3–8.
29. Silver FH, Shah RG. Measurement of mechanical properties of natural and engineered implants. *Adv Tissue Eng Regen Med Open Access*. 2016;1(1):20–25.
30. Crespo MA, Jimenez HJ, Deshmukh T, et al. In vivo determination of the human corneal elastic modulus using vibrational optical coherence tomography. *Transl Vis Sci Technol.* 2022;11(7):11.
31. Silver F, Kelkar N, Deshmukh T, Horvath I, Shah R. Mechano-vibrational spectroscopy of tissues and materials using vibrational optical

Downloaded from tvst.arvojournals.org on 05/05/2023

coherence tomography: A new non-invasive and non-destructive technique. *Recent Prog Mater.* 2020;2(2):1–16.

32. Silver FH, Shah R. "Virtual biopsies" of normal skin and thermal and chemical burn wounds. *Adv Skin Wound Care*. 2020;33:307–312.
33. Silver FH, Shah RG, Richard M, Benedetto D. Comparative "virtual biopsies" of normal skin and skin lesions using vibrational optical coherence tomography. *Skin Res Technol.* 2019;25:743–749.
34. Silver FH, Kelkar N, Deshmukh T, Ritter K, Ryan N, Nadiminti H. Characterization of the biomechanical properties of skin using vibrational optical coherence tomography: Do changes in the biomechanical properties of skin stroma reflect structural changes in the extracellular matrix of cancerous lesions? *Biomolecules.* 2021;11:1712.
35. Silver FH, Shah RG, Richard M, Benedetto D. Use of vibrational optical coherence tomography to image and characterize a squamous cell. *J Derm Res Ther.* 2019;5:1–8.
36. Sridhar MS. Anatomy of cornea and ocular surface. *Indian J Ophthalmol.* 2018;66:190–194.
37. Tsubota K, Mashima Y, Murata H, Sato N, Ogata T. Corneal epithelium in keratoconus. *Cornea*. 1995;14:77–83.
38. Bitirgen G, Ozkagnici A, Bozkurt B, Malik RA. In vivo corneal confocal microscopic analysis in patients with keratoconus. *Int J Ophthalmol.* 2015;8:534–539.
39. Mocan MC, Yilmaz PT, Irkec M, Orhan M. In vivo confocal microscopy for the evaluation of corneal microstructure in keratoconus. *Curr Eye Res.* 2008;33:933–939.
40. Weed KH, MacEwen CJ, Cox A, McGhee CN. Quantitative analysis of corneal microstructure in keratoconus utilising in vivo confocal microscopy. *Eye (Lond)*. 2007;21:614–623.
41. Silverman RH, Urs R, Roychoudhury A, Archer TJ, Gobbe M, Reinstein DZ. Epithelial remodeling as basis for machine-based identification of keratoconus. *Invest Ophthalmol Vis Sci*. 2014;55:1580–1587.

Downloaded from tvst.arvojournals.org on 05/05/2023